Accelerated Publications

The Antimalarial Drug Resistance Protein *Plasmodium falciparum* Chloroquine Resistance Transporter Binds Chloroquine†

Hanbang Zhang, Michelle Paguio, and Paul D. Roepe*

Department of Chemistry, Department of Biochemistry and Molecular Biology, and Lombardi Cancer Center, Georgetown University Medical Center, 3900 Reservoir Road, Washington, D.C. 20057

Received April 28, 2004; Revised Manuscript Received May 24, 2004

ABSTRACT: Recently, mutations in the novel polytopic integral membrane protein PfCRT were shown to cause chloroquine resistance (CQR) in the malarial parasite *Plasmodium falciparum*. PfCRT is not a member of the well-known family of ABC proteins that have previously been associated with other drug resistance phenomena. Thus, the mechanism(s) whereby mutant PfCRT molecules confer antimalarial drug resistance is (are) unknown. Previously, we succeeded in overexpressing PfCRT to high levels in *Pichia pastoris* yeast by synthesizing a codon-optimized version of the *pfcrt* gene. Using purified membranes and inside-out plasma membrane vesicles (ISOV) isolated from strains harboring either wild-type or CQR-associated mutant PfCRT, we now show that under deenergized conditions the PfCRT protein specifically binds the antimalarial drug chloroquine (CQ) with a K_D near 400 nM but does not measurably bind the related drug quinine (QN) at physiologically relevant concentrations. Transport studies using ISOV show that QN is passively accumulated as expected on the basis of previous measurement of the ISOV ΔpH for the different strains. However, passive accumulation of CQ is lower than expected for ISOV harboring mutant PfCRT, despite higher ΔpH for these ISOV.

Resistance to chloroquine (CQ)[1] and other antimalarial drugs is a global crisis. Well over a million die of *Plasmodium falciparum* malaria annually, and the spread of existing CQ-resistant (CQR) strains, as well as continued evolution of new CQR strains, greatly impedes management of the disease. Elucidating antimalarial drug resistance mechanisms at a molecular level is urgently required.

Nearly 10 years ago, a homologue of the well-known human MDR 1 protein [P-glycoprotein (Pgp)] was found in *P. falciparum* and named Pgp homologue 1 (Pgh-1) (*1*, *2*). A variety of data supported the idea that overexpression and/or mutation of Pgh-1 perhaps conferred CQR (reviewed in ref *3*). However, early on Wellems and colleagues found that the chromosomal locus that segregated with CQR phenotypes in progeny from a *P. falciparum* genetic cross did not contain the *Pgh-1* gene (*4*). Subsequently (*5*, *6*), it was found that mutations in the *pfcrt* gene segregated with, and caused, the verapamil (VPL) reversible CQR phenotype. Mutations in Pgh-1 appear to be involved in modulating mild resistance to related quinoline antimalarials such as mefloquine (MQ) (*7*) but do not confer CQR in and of themselves. PfCRT is found in the digestive vacuolar (DV) membrane of the malarial parasite (*5*) where it likely performs some yet to be defined membrane transport function (*3*, *8*−*10*).

Different patterns of *pfcrt* mutations confer CQR in malarial parasite isolates from different regions of the globe. Perhaps the most heavily studied mutant (CQR-associated) PfCRT molecule is the Dd2 isoform (*6*, *9*, *10*), which is encoded by an allele commonly found in drug-resistant African and southeast Asian *P. falciparum* isolates. Dd2 harbors seven point mutations relative to a common allele associated with CQ-sensitive (CQS) parasites, the HB3 allele, whereas the 7G8 (South American) allele associated with CQR harbors five PfCRT point mutations (*5*). It is not known how these different patterns of mutations contribute to the different antimalarial drug resistance phenotypes seen in these strains. Similar to the case of hu MDR 1 mediated drug resistance for tumor cells (*11*), selection of various parasite strains with different drugs, drug combinations, and/or different culture conditions complicates interpretation. Thus, molecular biochemical studies of recombinant PfCRT proteins under controlled conditions would greatly assist progress.

However, heterologous expression of malarial genes, particularly those encoding large integral membrane proteins, is extraordinarily difficult, if not impossible, via conventional means because of their very high (65−85%) AT base pair content. This impedes molecular biochemical studies of many important malarial transporters. Recently, we "back-trans-

† Supported by NIH Grants AI56312 and AI45759 to P.D.R.

* To whom correspondence should be addressed: tel, 202-687-7300; fax, 202-687-6209; e-mail, roepep@georgetown.edu.

[1] Abbreviations: PfCRT, *Plasmodium falciparum* chloroquine resistance transporter; CQR, chloroquine resistance (resistant); ISOV, inside-out plasma membrane vesicles; CQ, chloroquine; QN, quinine; MDR, multidrug resistance; Pgp, P-glycoprotein; Pgh-1, Pgp homologue 1; MQ, mefloquine; DV, digestive vacuole; CQS, chloroquine sensitive; BSA, bovine serum albumin; ABC, ATP-binding cassette.

10.1021/bi049137i CCC: $27.50
Published on Web 06/10/2004

lated" endogenous wild-type PfCRT to construct a synthetic gene that was in theory optimal for high level expression in yeast (*10*). This synthetic gene was fused to a fragment encoding a biotin acceptor domain, constitutively expressed in *Saccharomaycs cerevisiae*, and inducibly expressed to higher levels in *Pichia pastoris.* In both cases, much of the protein was well localized to the plasma membrane of these yeast.

Also, using single cell photometry methods and living intraerythrocytic parasites, we have previously measured lower digestive vacuolar (DV) pH for CQR malarial parasites (*9*, *12*). On the basis of these data and our initial studies with recombinant PfCRT (*10*), we proposed that mutant PfCRT perturbs DV pH regulation, either by modulating the activity of the endogenous DV membrane V-type ATPase or by acting as a Cl^- channel (*10*). These pH perturbations will differentially influence resistance to various quinoline antimalarials (e.g., CQ, QN, and MQ), since the weakly basic drugs have different pK_a values and different pH-dependent heme binding (8). For example, weak base N pK_a values are 5.1 and 9.8 for QN but 8.4 and 10.1 for CQ, predicting that all DV localized CQ is 2+, whereas considerable QN is 1+. Thus, PfCRT-instigated changes in DV pH have different relative effects on accumulation and retention of the compounds, as well as their binding to DV heme and perhaps other molecules (*8*). In this report, we show that this model for PfCRT should now be modified to include direct interaction with at least one antimalarial drug, the 7-chloro-4-aminoquinoline CQ.

MATERIALS AND METHODS

Materials. All oligonucleotides, plasmid DNA constructs, bacterial and yeast strains, and growth media were as described previously (*10*). Rabbit anti-PfCRT IgG was a kind gift of the Wellems laboratory (NIAID, NIH, Bethesda, MD). HRP-conjugated anti-rabbit IgG, HRP-conjugated strepavidin, and ECL detection reagents were from Amersham. Zymolase-20T was from ICN, and [^{3}H]CQ (5.0 Ci/mmol) and [^{3}H]QN (50.0 Ci/mmol) were from American Radiolabelled Chemicals Inc. All other chemicals were of reagent grade or better and were purchased from commercial sources.

Yeast Strains and Fractionation. P. pastoris yeast was transformed by the lithium acetate method with 2 μg of target pPIC3.5/crt-bad plasmid DNA (*10*) and 10 μg of carrier plasmid. Transformants were selected on minimal medium lacking histidine. Single colonies were picked, archived, and grown as described (*10*). PfCRT expression was induced in these strains by 24 h growth in the presence of 0.5% MeOH as the sole carbon source. Previously, we have noted that Dd2 and HB3 PfCRT isoforms fold and/or insert into yeast plasma membranes with slightly different kinetics (*10*). However, at 24 h, expression and plasma membrane insertion for both have plateaued and are equal (see Results).

Yeast was fractionated, and membranes or ISOV were isolated and purified as described previously (*10*, *13*). Protein content in these preparations was repeatedly quantified, multiple times by multiple personnel, using the amido black assay. Any possible variation in protein quantification due to detergents and/or other reagents used in the purifications was accounted for in the BSA protein standards. Equivalent [PfCRT]/μg of total membrane protein for different samples was confirmed by Western blot titration (see Results).

Analysis of Drug Binding and Transport. We attempted several methods for analyzing drug binding to membrane fragments or ISOV. Filtration-based assays tended to give high background due to hydrophobic drug adhering to the filters. We thus quantified binding to membranes using a centrifugation-based assay. Briefly, membranes (75 μg of protein) were suspended in 100 μL of assay buffer [10 mM MES (pH 6.5)/140 mM KCl/330 mM sucrose/4 mM $MgCl_2$/1 mM DTT] in polyallomer tubes and incubated with various concentrations of radiolabeled drug (see Results), in the presence or absence of a 200-fold excess of cold (unlabeled) drug to block specific binding (see Results). The tubes were centrifuged in an air-driven microfuge to collect the membranes, and pellets were washed once with 100 μL of ice-cold assay buffer. Washed pellets were transferred to scintillation vials via cutting the bottom of the polyallomar tube, 14 mL of Ecoscint A scintillation liquid was added, and radioactivity was quantified using a Beckman LS6500 liquid scintillation counter.

Measurement of the steady-state accumulation of drugs into ISOV was done in similar buffer but with the pH adjusted to 7.8 for CQ and 6.5 for QN (to reflect their unequal pK_a at the quinolinal N).[2] ISOV protein (50 μg) was mixed with 50 nM drug and buffer either with or without 2 mM ATP. Aliquots were either immediately quenched with ice-cold buffer and filtered (zero accumulation control) or incubated for 20 min, quenched, and then filtered. Trapped radioactivity was quantified as above. These assays provided steady-state accumulation data but proved inadequate for monitoring the kinetics of drug transport in any detail.

Thus, to test conclusions from steady-state accumulation assays and to analyze transport kinetics, we also used flow dialysis methods as described (*14*, *15*). The 20000 MW cutoff dialysis membrane was placed between the upper and lower chambers of a custom-made flow dialysis chamber. The lower chamber was purged with 10 mL of 50% EtOH, then 10 mL of distilled water, and then 10 mL of transport buffer [10 mM MES−Tris (pH 6.5−7.8)/140 mM KCl/330 mM sucrose/4 mM $MgCl_2$/1 mM DTT]. Purified ISOV (500 μg) were added to the upper chamber, and the mixture was continuously stirred. The flow rate through the lower chamber was 2.1 mL/min, and dialysate was collected at a rate of 1 mL/fraction. Radiolabeled drug (200 nM final concentration) was added to the upper chamber, and the mixture was equilibrated until the rate of substrate dialysis renormalized (*14*). Transport of weak base drug into the ISOV was initiated by the addition of 2 mM ATP to acidify the ISOV interior and was reversed by addition of 20 μM protonophore FCCP (see Results).

[2] Accumulation of both weakly dibasic drugs is expected to be passive and controlled by the ΔpH formed upon activation of the endogenous H^+ ATPase (*8*). Diffusion of the neutral drug is much faster than that of the singly charged drug, which is much faster than that of the doubly charged drug. The hydrolysis activity of the H^+ ATPase is relatively constant pH 6.5−7.8, but the second pK_a of CQ vs QN differs. So we adjusted the buffer pH to bias toward similar (neutral drug), CQ vs QN, without perturbing ATPase activity, so that the CQ vs QN accumulation data would be more directly comparable. Regardless, for either drug alone, the relative differences seen for the different ISOV are similar pH 6.5−7.8.

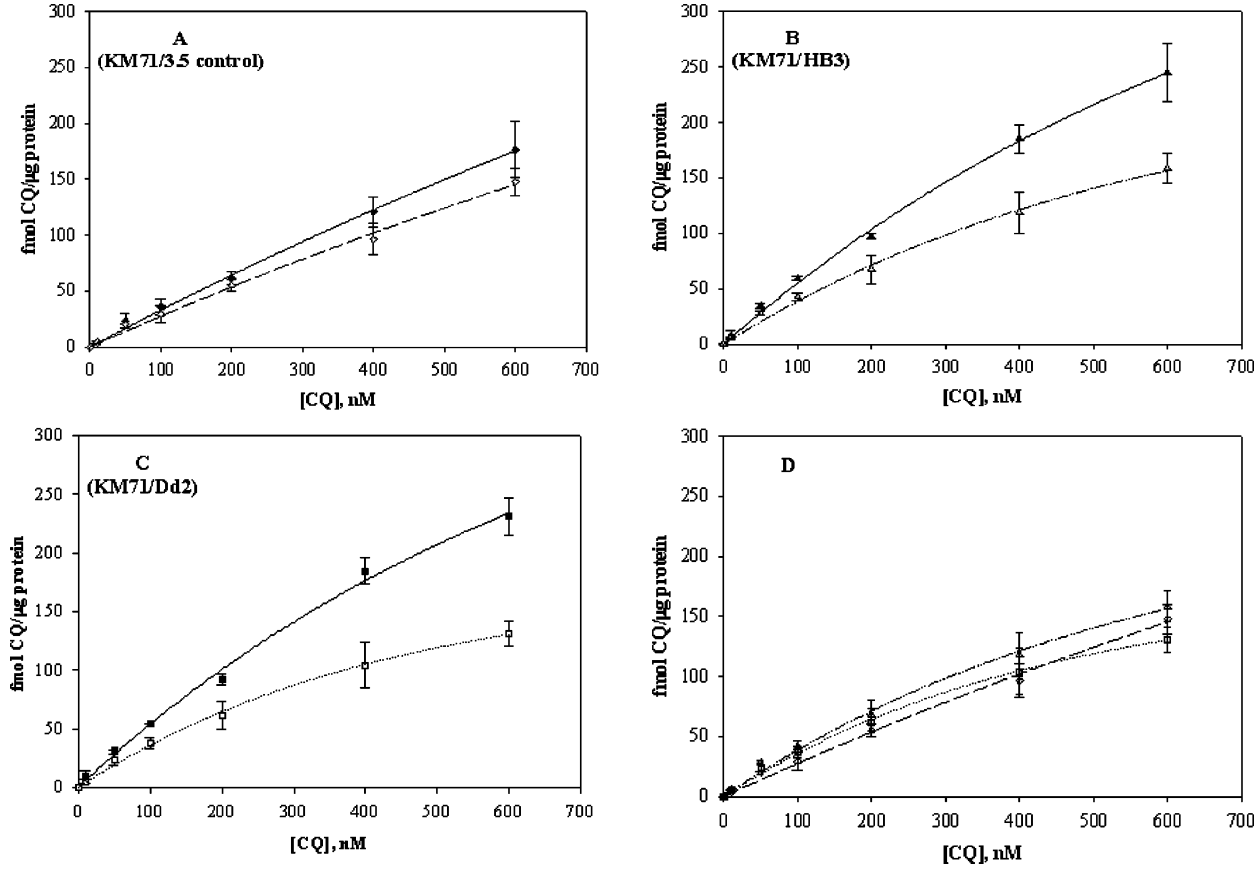

FIGURE 1: CQ binding to KM71/3.5 (A), KM71/HB3 (B), and KM71/Dd2 (C) yeast membranes harboring no PfCRT, wild-type PfCRT, or CQR-associated mutant PfCRT, respectively. A centrifugation-based assay (see Materials and Methods) was used to quantify binding. At least four samples were used at each concentration of CQ, using multiple membrane preparations harboring equivalent [PfCRT] and/or [membrane protein] (e.g., see Figure 3). Each sample contained 75 μg of membrane protein. In each panel are shown the results from two series: solid symbols (solid lines) are data (±SD) for membranes incubated with radiolabeled drug alone (=total binding); open symbols (dashed lines) are data for membranes incubated with radiolabeled drug at the same concentrations plus a 200-fold molar excess of cold (unlabeled) drug to reveal nonspecific binding. Panels A−C are summarized data for the three strains, and panel D overlays the equivalent nonspecific binding for all three strains. Each data set is fit by a single exponential, $R^2 > 0.98$ in each case. Relative binding among the samples was similar ± 2 mM ATP (data not shown).

RESULTS

Results of [^{3}H]CQ equilibrium binding assays are summarized in Figure 1. We examined binding over physiologically relevant concentrations of CQ (see Discussion). Strain KM71/3.5 (diamonds, Figure 1A) is a control strain that is grown and induced in a similar fashion but does not harbor PfCRT (*10*). Strain KM71/Dd2 (squares, Figure 1C) expresses CQR-associated PfCRT harboring seven mutations (M74I, N75E, K76T, A220S, Q271E, N326S, R371I) relative to CQS-associated HB3 (strain KM71/HB3; triangles, Figure 1B). [^{3}H]CQ binding to Dd2 (Figure 1C) and HB3 membranes (Figure 1B) is markedly higher in the absence of a 200-fold molar excess of cold CQ (solid symbols) relative to the presence (open symbols), whereas binding in the presence or absence of cold CQ is statistically the same for control strain KM71/3.5 (Figure 1A). Background (nonspecific) binding to all three membrane preparations is similar (Figure 1D). Subtracting background binding (Figure 1D) from total binding measured in the absence of excess cold competitor (Figure 1B,C) yields specific binding to HB3 (triangles) or Dd2 (squares) PfCRT over this concentration range (Figure 2A). Scatchard transformation of the data (Figure 2B) reproducibly suggests that the affinity of CQ for Dd2 PfCRT (385 nM) may be slightly higher than that measured for HB3 PfCRT (435 nM); however, note that propagation of standard deviation for the raw data used to calculate affinity (i.e., Figure 1B−D) does not currently allow for a statistically rigorous distinction between these affinities. Nonetheless, extrapolation of the data to the ordinate gives a B_{max} of approximately 162 and 137 fmol of CQ/μg of membrane protein for KM71/HB3 and KM71/Dd2 membranes, respectively. Previous work (*10*) suggests that approximately 1% of the protein in these membranes is PfCRT. Using the calculated molecular mass of 57.7 kDa for biotinylated PfCRT (*10*), this yields 175 fmol of PfCRT/μg of membrane protein. Thus, importantly, apparent binding to PfCRT is near 1:1 molar stoichiometry at these CQ concentrations and exhibits meaningful affinity (see Discussion).

However, for reliable interpretation of these data, it is crucial that equivalent concentrations of HB3 vs Dd2 PfCRT be present in different yeast membrane samples and that total membrane protein content for 3.5 vs HB3 vs Dd2 samples be equivalent. Along with multiple amido black assays to control for the latter, we also electrophoresed all samples used in these experiments side by side and quantified biotinylated PfCRT as well as endogenously biotinylated yeast membrane proteins by avidin−HRP detection and

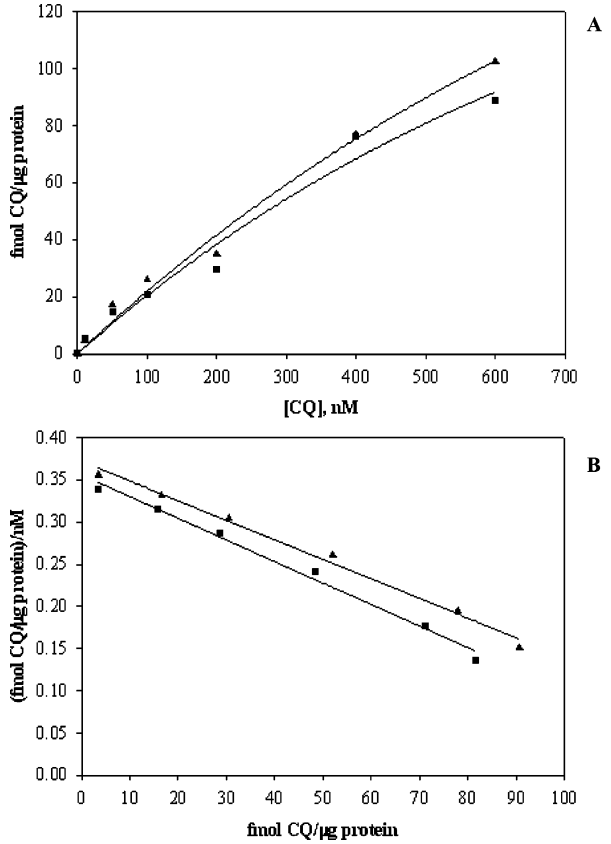

FIGURE 2: Net CQ binding to wild-type and CQR-associated mutant PfCRT. (A) Nonspecific binding (Figure 1D) was subtracted from total binding for KM71/HB3 and KM71/Dd2 membranes (Figure 1B,C, solid lines) to reveal specific binding to PfCRT. Solid squares are data for Dd2, and solid triangles are data for HB3. (B) Net specific binding (panel A) was fit to a single exponential [$y = a(1 - e^{-bx})$] and converted to Scatchard format. From these plots, computed K_d (nM) and B_{max} (fmol of CQ/μg of membrane protein) were 435 and 162 for HB3 PfCRT and 385 and 137 for Dd2 PfCRT, respectively.

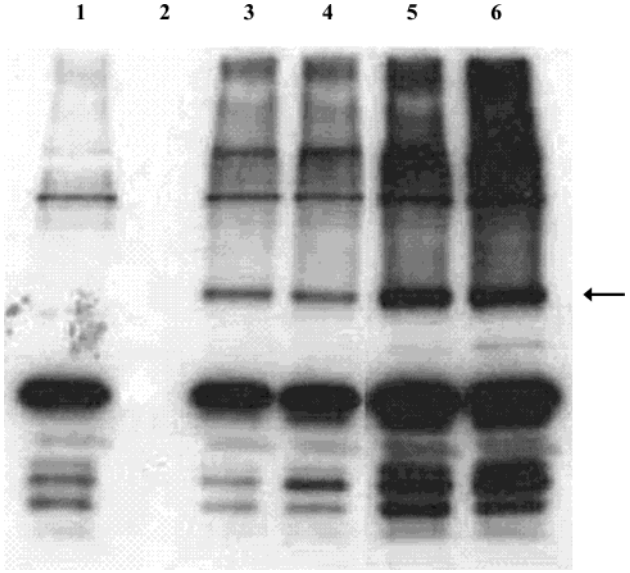

FIGURE 3: Comparison of relative membrane protein and PfCRT expression for different membranes used in the binding assays. Isolated membranes used in the drug binding assay were analyzed for protein content by the amido black assay (see Materials and Methods), equivalent aliquots were also electrophoresed and transferred to nitrocellulose, and biotinylated proteins were detected with HRP−avidin as described (*10*). Lanes 1, 3, and 4 are 10 μg of one batch of KM71/3.5, KM71/HB3, and KM71/Dd2 membranes, respectively. Correspondence between the concentration of total membrane protein (via amido black) and endogenously biotinylated yeast membrane proteins (via densitometry of the common biotinylated protein bands) is excellent. Lanes 5 and 6 are 20 μg of a second batch (independent isolation) of KM71/HB3 and KM71/Dd2 membranes, respectively. Again, as also the case in comparing lanes 3 and 4, equivalent protein and equivalent [PfCRT] (marked with the arrow) are found for these samples. Similar analysis for ISOV preparations (not shown) revealed similar equivalence among the ISOV preparations.

densitometry (e.g., Figure 3). Endogenously biotinylated yeast membrane proteins offer convenient confirmation of equivalent [total membrane protein] for different samples. Combining data such as those in Figure 3 with data as in Figures 1 and 2 allows us to conclude that the altered apparent affinity for specific binding of CQ is due to PfCRT mutations and is not a consequence of dramatically different levels of heterologously expressed proteins.

Via analysis similar to that above and shown in Figures 1−3, we could detect no specific binding of the related quinoline antimalarial drug quinine (QN) to any of these samples (data not shown). Our interpretation of this key result is offered in the Discussion.

We next analyzed accumulation of [^{3}H]CQ and [^{3}H]QN into inside-out plasma membrane vesicles (ISOV) created from these strains as described (*10*). To a first approximation, ISOV mimic the bioenergetics of the digestive vacuole (DV), the normal membrane host of PfCRT. Both harbor a H^+ ATPase capable of acidifying their interiors by 1.5−2.5 units upon the addition of external ATP. Since CQ and QN are weakly basic hydrophobic drugs, they should accumulate within the interior of ISOV in response to the transmembrane ΔpH formed upon addition of ATP (*10*), similar to what occurs in the living parasite DV. Moreover, since Dd2 PfCRT ISOV generate a higher ΔpH (acid inside) relative to ISOV produced from the other strains (*10*), then via the predictions of the Henderson−Hasselbach equation we expect accumulation of both drugs to be significantly higher for Dd2 ISOV, as described in detail elsewhere (*8*).

Indeed, as shown in Figure 4A, steady-state QN accumulation at 20 min for all samples is dependent upon the addition of ATP and is also fully dissipated upon the addition of the protonophore FCCP (not shown). As expected (*8*, *10*) accumulation of QN is higher for Dd2 ISOV relative to the other strains. The approximately 40% additional accumulation actually corresponds quite closely to what is predicted on the basis of quantification of the increased ΔpH for Dd2 ISOV (*8*, *10*). However, notably, CQ accumulation for Dd2 ISOV is conspicuously *lower* than predicted as measured by a similar filtration assay (Figure 4B).

To test this conclusion further, we also analyzed transport by a complementary flow dialysis method (*14*) that has better kinetic resolution and that is less complicated by high background binding of drug to membranes and/or filters (Figure 5). Accumulation into the ISOV is initiated by addition of 2 mM ATP (first arrow) and dissipated by addition of 20 μM protonophore (second arrow). Again, as shown in Figure 5, steady-state QN accumulation (panel A) is higher in Dd2 ISOV (closed squares) relative to the other samples as predicted on the basis of weak base partitioning theory (*8*). However, CQ accumulation (panel B) is again

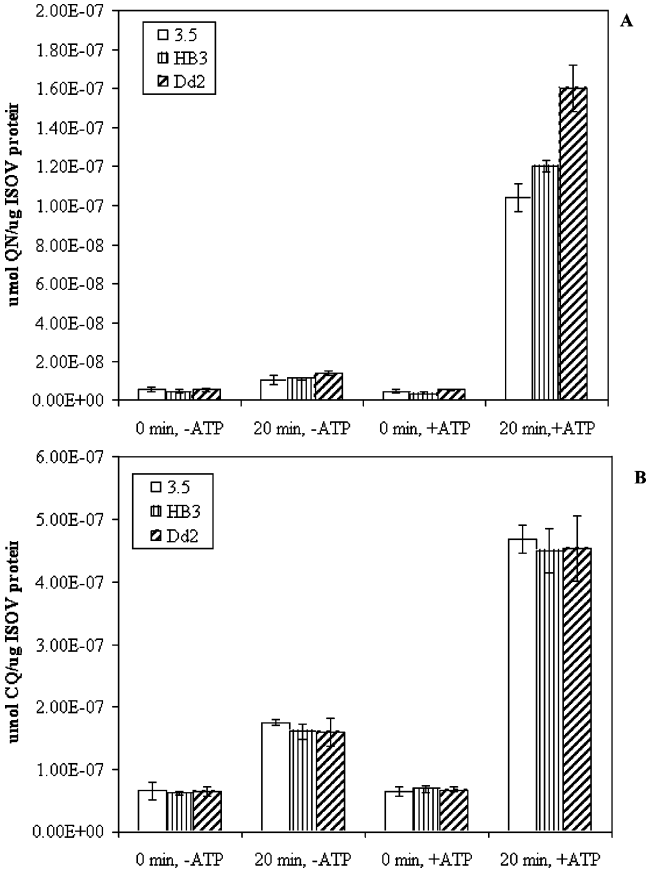

FIGURE 4: Steady-state [^{3}H]QN and [^{3}H]CQ accumulation into yeast ISOV. ISOV (50 μg) were incubated in 500 μL of transport buffer plus 50 nM drug (A, QN; B, CQ) as described in Materials and Methods. Open bars: KM71/3.5. Striped bars: KM71/HB3. Hashed bars: KM71/Dd2. ATP (2 mM) was added to activate the endogenous H^+ ATPase and thus initiate accumulation of the weak base drugs. Zero accumulation controls had 2 mL of ice-cold transport buffer added immediately to quench the reaction. After incubation, ISOV were filtered through GF/F glass microfiber filters, washed twice with 2 mL of ice-cold transport buffer, and placed in scintillation vials, and radioactivity was quantified by scintillation counting. In each case the data shown are the average of more than four determinations ($\pm$SD) using multiple independent ISOV preparations as shown in Figure 3. For both QN and CQ, there is some degree of background (nonspecific) binding of drug to ISOV membranes that is time dependent (compare 0 min minus ATP vs 20 min minus ATP), yet there is also significant accumulation into ISOV that is clearly in response to generation of an acid inside ΔpH (right-hand side, panels A and B). For QN (A), net accumulation in the different ISOV is proportional to the magnitude of ΔpH generated for these ISOV (*10*), but for CQ (B) accumulation is conspicuously lower than expected for KM71/Dd2.

notably lower than predicted for Dd2 ISOV. Additionally, the rate of CQ accumulation in the Dd2 ISOV (which is better revealed in these flow dialysis experiments) is conspicuously slower relative to either control 3.5 or HBS ISOV (see legend). Also, note that accumulation of CQ for Dd2 ISOV is conspicuously slower than accumulation of QN or the generation of a ΔpH (*10*) for identical Dd2 ISOV under similar conditions.

DISCUSSION

Analysis of how membrane proteins linked to drug resistance phenomena might interact with drugs is a major area of investigation. In the case of well-characterized ABC transporters previously linked to drug resistance (e.g., hu MDR 1 vs tumor multidrug resistance), Scatchard plot analyses that precisely quantify specific binding of any hydrophobic drugs to these transporters are rare. Thus, although a variety of data have been published that suggest some type of interaction between some drugs and hu MDR 1 or its relatives (including malarial parasite Pgh-1), binding affinities for many drugs, as well as the thermodynamics and kinetics of any postulated drug transport, remain unclear. In part, this is because high background association of hydrophobic drugs to membranes greatly complicates quantification of their binding to membranes and/or transport across membranes. In general, the more hydrophobic the drug, the greater the potential experimental difficulty for both binding and transport measurements.

However, in the case of the recently discovered novel protein PfCRT vs CQ, the data are more clear-cut. Even though substantial background (nonspecific) binding to membranes is also observed in this case, CQ is not quite as hydrophobic as many of the drugs that are believed to bind to hu MDR 1 and/or its ABC transporter homologues [log *P*(CQ) is near 1 under physiologic conditions]. Also, wild-type vs mutant PfCRT have been inducibly overexpressed to high levels in yeast (*10*). Thus, despite high nonspecific membrane binding, Scatchard analysis of [^{3}H]CQ binding to very well controlled yeast membrane samples harboring equivalent protein and equivalent [PfCRT] reveals specific binding to wild-type and mutant PfCRT at meaningful affinity and stoichiometry. Importantly, although the external (extraerythrocytic) [CQ] is typically a few nanomolar in culture or in plasma, estimates for [CQ] in the DV (where it acts to inhibit heme processing) range from 10^2- to 10^4-fold higher than external (under physiologic conditions; see ref *8*). Thus, interestingly, the affinities we measure here are likely relevant for interaction of CQ with the internal (intra-DV) face of PfCRT but perhaps not the external (cytosolic) face, where [CQ] under physiologic conditions would only be several nanomolar (*8*).

In contrast, at least at these physiologically relevant concentrations, the related drug QN does not specifically bind to either PfCRT isoform. This might seem paradoxical since *P. falciparum* strain Dd2 (which harbors the Dd2 mutant PfCRT studied here) is resistant to both CQ and QN. However, recent allelic exchange experiments using a CQS strain (*6*) show that expression of the Dd2 allele in and of itself recapitulates CQR seen in the laboratory strain Dd2 but does not promote QNR. Presumably, QNR requires additional physiologic or genetic events along with expression of mutant PfCRT. Indeed, QNR may in fact be linked to polymorphisms in the single Na^+/H^+ exchanger isoform known to exist on *P. falciparum* chromosome 13 (M. Ferdig and T. Wellems, personal communication). Presumably, additional drug exposure and/or other facets to the history of laboratory strain Dd2 add with PfCRT mutations to confer a "multidrug resistance" phenotype that likely has several genetic contributions.

The transport data obtained either by centrifugation or by flow dialysis assays are interesting. Transport and accumulation of QN and CQ are similar for KM71/3.5 control vs KM71/HB3 ISOV, as would be predicted, since previous work showed that these ISOV preparations maintained similar ΔpH upon addition of ATP (*10*). Since these drugs

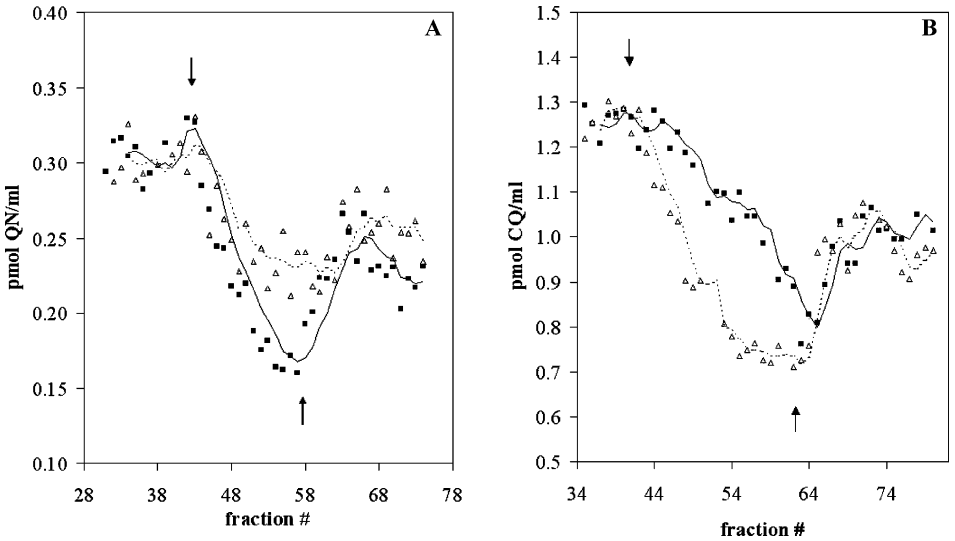

FIGURE 5: Kinetics of [^{3}H]QN (A, left panel) and [^{3}H]CQ (B, right panel) accumulation into ISOV measured via flow dialysis. The hydrophobicity of CQ and QN makes filtration-based transport assays difficult; thus we also used flow dialysis to monitor the kinetics of accumulation and to verify relative steady-state accumulation as measured by filtration (Figure 4). Shown are the average of two representative experiments for KM71/3.5 (open triangles) and KM71/Dd2 (closed squares) ISOV. KM71/HB3 ISOV gave data nearly identical to those for KM71/3.5 (not shown) and were thus omitted for clarity of presentation. The flow rate was set at 2.1 mL/min in all cases via a peristaltic pump, and 1 mL dialysate fractions were collected. Assays were initiated by adding 500 μg of ISOV to the upper chamber, which had been preequilibrated with assay buffer plus 200 nM radiolabeled drug. After the plateau 2 mM ATP was added to the upper chamber to acidify the ISOV interior and initiate accumulation of the weak base drug (first arrow). After 20 fractions were collected, FCCP was added to collapse ΔpH and release accumulated drug (second arrow). Note the excellent agreement between relative steady-state QN and CQ accumulation for the ISOV in this assay vs the filtration assay (Figure 4). Again, QN accumulation is higher for KM71/Dd2 as is expected, but CQ accumulation (using the very same ISOV) is conspicuously lower than expected. Moreover, the flow dialysis data reveal a markedly slower rate of accumulation for KM71/Dd2 ISOV vs control (B) or vs KM71/HB3 (not shown), which was again nearly identical to control KM71/3.5 and thus omitted for clarity of presentation.

are weak bases, they are expected to accumulate within acid compartments such as the interior of energized ISOV via the predictions of the Henderson−Hasselbach equation (*8*). If the magnitude of pH gradients is similar between two vesicle preparations (as is the case for 3.5 vs HB3 ISOV upon addition of ATP; see ref *10*), then accumulation is expected to be similar as we indeed observe.

Transport of QN into KM71/Dd2 ISOV is to a higher steady state than that for either the 3.5 or HB3 ISOV preparations, but within our ability to measure is via a similar rate constant (e.g., rates of accumulation in Figure 5A are similar). This is also as expected, since these Dd2 ISOV maintain a conspicuously higher ΔpH upon addition of ATP (*10*), and QN accumulation into the ISOV is expected to be via passive diffusion. AO partitioning data that reveal ΔpH for these ISOV (*10*) are difficult to quantify precisely, so it is not possible to calculate whether the increased QN accumulation that is observed is exactly as would be predicted on the basis of strict application of Henderson−Hasselbach theory (*8*). However, if we reasonably assume that there is a logarithmic relationship between AO response vs formed ISOV ΔpH, then we expect an approximately 40% increase in steady-state passive QN accumulation for Dd2 ISOV, as is indeed observed (Figures 4 and 5). Thus, relative accumulation of QN in the three ISOV preparations, along with previous data (*10*), suggests that QN accumulation is passive and that it equilibrates in response to ΔpH formed upon addition of ATP (*8*). Along with a lack of any evidence for direct binding of QN to either PfCRT isoform, we conclude that both wild-type and the CQR-associated mutant PfCRT do not directly interact with QN.

In contrast, notably, we also expect an (even greater) net increase in CQ accumulation for KM71/Dd2 ISOV relative to 3.5 or HB3 ISOV. However, we actually find *less* than expected accumulation of CQ for Dd2 ISOV. Lower than expected accumulation at significantly slower rate occurs despite formation of a higher ΔpH (acid inside) across these ISOV membranes upon addition of ATP (*10*). At this lower internal ISOV pH, virtually all concentrated CQ entrapped within the ISOV is expected to be in the doubly protonated state at any given instant, whereas significant external CQ will be singly charged. That is, there is a concentration gradient in CQ++ oriented outward. Thus, to explain reduced CQ accumulation for Dd2 ISOV, one possibility is that mutant PfCRT catalyzes downhill facilitated diffusion of CQ++ molecules out of the ISOV. However, there is also a large gradient in H^+ oriented outward under these conditions, so another possibility is that mutant PfCRT performs H^+- (or perhaps HCO_3^-- or Cl^--) coupled active transport of CQ+ in the outward direction. Either scenario could in theory reduce net expected accumulation in the ISOV as is observed. Also, either scenario would contribute to lower net CQ accumulation within the parasite DV as is typically observed for CQR strains.

With regard to the second possibility, we note that mutation of PfCRT also causes pH DV changes (*9*, *10*, *12*). These pH changes influence resistance to CQ and other heme-acting antimalarial drugs because their interaction(s) with heme target(s) is (are) highly pH dependent (*8*, *16*). In a general way, an ion-coupled CQ+ transport model provides an attractive basis for explaining the reduced passive accumulation of CQ shown here, as well as DV acidification measured previously (*9*, *12*). The endogenous transport activity of wild-type PfCRT is currently unknown, but if PfCRT is an active transporter, this transport would likely be ion-coupled since a high ΔpH exists across

the endogenous DV membrane and since there is no generation of ATP within the DV. With two regions harboring basic N that can assume several conformations, CQ might partially mimic the structure of certain amino acids as they are released upon hemoglobin digestion within the DV. These amino acids (or peptides containing them) must be exported from the parasite DV to the cytosol via some yet to be defined transport process. So we could speculate that CQ transport via mutant PfCRT represents a modified endogenous amino acid transport function of the wild-type transporter, with the spectrum of Dd2 PfCRT mutations allowing for better recognition of CQ.

Regardless of how intuitively attractive this scenario might be, a variety of additional extensive transport and binding studies (particularly with purified, reconstituted PfCRT protein) are needed to firmly distinguish between these and additional possibilities. Additional studies, using a variety of drugs and a variety of the different mutant PfCRT isoforms now known to exist, will elucidate how specific PfCRT mutations affect resistance (or sensitivity) to the array of quinoline-based antimalarial drugs currently in use. In this regard, studies at a variety of pHs (to account for the range of pK_a found in this class of drugs) will be particularly important. Such information will be useful in designing more effective antimalarial therapy.

ACKNOWLEDGMENT

We thank our laboratory colleagues T. Bennett and L. Amoah for assistance and Drs. M. Ferdig (University of Notre Dame), R. Cooper (Old Dominion College), B. Adams (NIH), T. Wellems (NIH), and D. Fidock (Albert Einstein College of Medicine) for helpful conversations. This paper is dedicated to Mary Hoffman Shaw.

REFERENCES

1. Foote, S. J., Thompson, J. K., Cowman, A. F., and Kemp, D. J. (1989) Amplification of the Multidrug Resistance Gene in Some Chloroquine-Resistant Isolates of *P. falciparum*, *Cell 57*, 921−930.
2. Wilson, C. M., Serrano, A. E., Wasley, A., Bogenschutz, M. P., Shankar, A. H., and Wirth, D. F. (1989) Amplification of a Gene Related to Mammalian mdr Genes in Drug-Resistant *Plasmodium falciparum*, *Science 244*, 1184−1186.
3. Howard, E., Zhang, H., and Roepe, P. D. (2002) A Novel Transporter, Pfcrt, Controls Antimalarial Drug Resistance, *J. Membr. Biol. 190*, 1−8.
4. Wellems, T. E., Panton, L. J., Gluzman, I. Y., do Rosario, V. E., Gwadz, R. W., Walker-Jonah A., and Krogstad, D. J. (1990) Chloroquine Resistance not Linked to *mdr*-like Genes in a *Plasmodium falciparum* Cross, *Nature 345*, 253−255.
5. Fidock, D. A., Nomura, T., Talley, A. K., Cooper, R. A., Dzekunov, S. D., Ferdig, M. T., Ursos, L. M. B., Su, X.-z., Wooton, J. C., Roepe, P. D., and Wellems, T. E. (2000) Mutations in the Digestive Vacuole Transmembrane Protein PfCRT and Evidence for Their Role in Chloroquine Resistance, *Mol. Cell 6*, 861−871.
6. Sidhu, A. B., Verdier-Pinard, D., and Fidock, D. A. (2002) Chloroquine Resistance in *Plasmodium falciparum* Malaria Parasites Conferred by Pfcrt Mutations, *Science 298*, 210, 213.
7. Reed, M. B., Saliba, K. J., Caruana, S. R., Kirk, K., and Cowman, A. F. (2000) Pgh1 Modulates Sensitivity and Resistance to Multiple Antimalarials in *Plasmodium falciparum*, *Nature 403*, 906−909.
8. Ursos, L. M. B., and Roepe, P. D. (2002) Recent Progress in Elucidating the Molecular Mechanism of Resistance to the Antimalarial Drug Chloroquine, *Med. Res. Rev. 22*, 465−491.
9. Bennett, T. N., Kosar, A. D., Ursos, L. M. B., Dzekunov, S., Sidhu, A. B. S., Fidock, D. A., and Roepe, P. D. (2004) Acidic Digestive Vacuolar pH of Drug Resistant *Plasmodium falciparum*, *Mol. Biochem. Parasitol. 133*, 99−114.
10. Zhang, H., Howard, E. M., and Roepe, P. D. (2002) Analysis of the Antimalarial Drug Resistance Protein PfCRT Expressed in Yeast, *J. Biol. Chem. 277*, 49767−49775.
11. Roepe, P. D. (2000) What is the Precise Role of Human MDR 1 Protein in Chemotherapeutic Drug Resistance? *Curr. Pharm. Des. 6*, 241−260.
12. Dzekunov, S., Ursos, L., and Roepe, P. D. (2000) Digestive Vacuolar pH of Intact Intraerythrocytic *P. falciparum* Either Sensitive or Resistant to Chloroquine, *Mol. Biochem. Parasitol. 110*, 107−124.
13. Fritz, F., Howard, E. M., Hoffman, M. M., and Roepe, P. D. (1999) Evidence for Altered Ion Transport in *S. cerevisiae* Overexpressing Human MDR 1 Protein, *Biochemistry 38*, 4214−4226.
14. Colowick, S. P., and Womack, F. C. (1969) Binding of Diffusible Molecules by Macromolecules: Rapid Measurement by Rate of Dialysis, *J. Biol. Chem. 244*, 774−777.
15. Roepe, P. D., and Kaback, H. R. (1989) Characterization and Functional Reconstitution of a Water Soluble Form of the Hydrophobic Membrane Protein *Lac* Permease, *Proc. Natl. Acad. Sci. U.S.A. 86*, 6087−6092.
16. de Dios, A. C., Tycko, R., Ursos, L. M. B., and Roepe, P. D. (2003) NMR Studies of Chloroquine−Ferriprotoporphyrin IX Complex, *J. Phys. Chem. A 107*, 5821−5825.

BI049137I